Jurnal Elektronika dan Telekomunikasi (JET), Vol. 22, No. 1, August 2022, pp. 30-39
Accredited by KEMDIKBUDRISTEK, Decree No: **158/E/KPT/2021**
doi: 10.55981/jet.460

Wireless Temperature Measurement Validation Method for PCR Machines by Magnetic Hall-Effect Sensor

Swivano Agmal[a, *], Jalu Ahmad Prakosa[b], Agus Sukarto Wismogroho[c]

[a]Research Center for Quantum Physics
National Research and Innovation Agency (BRIN)
Building 441-442, Puspiptek
Tangerang Selatan, Indonesia
[b]Research Center for Photonics
National Research and Innovation Agency (BRIN)
Building 441-442, Puspiptek
Tangerang Selatan, Indonesia
[c]Research Center for Advanced Material
National Research and Innovation Agency (BRIN)
Building 441-442, Puspiptek
Tangerang Selatan, Indonesia

Abstract

The temperature validation controlled by temperature indication has a vital role in the polymerase chain reaction (PCR) test machine or thermal cycler. However, the validation process is complicated for several types of thermal cycler. Some PCR test machines must close the lid tightly while running. It makes the probe's cable of the temperature sensor might be pinched or break when the thermal cycler lid is closed. Opening the lid (open-air condition) makes the measurement will not accurate. To solve this problem, wireless temperature measurement and validation methods for PCR machines are developed based on magnetic field measurements. The magnetic field of the object will respond to any changes in temperature. The hall-effect sensor, which is validated by gauss meter, detects any magnetic response a certain material covers even the object. This detection yields output data processed to find the thermal cycler's appropriate temperature wireless validation method. The experiment used a Neodymium magnet as a wireless probe. The position of the Neodymium magnet pole significantly affected the relation between magnetic flux and temperature in experimental results. The reversed pole toward sensors had better linearity (R^2= 0.8062) than the unreversed pole (R^2= 0.7794). The annealing step commonly achieved the optimum measurement uncertainty. However, the measurement uncertainty and signal sensitivity investigation recommended employing the beneficial combination of pole magnet position to design the temperature validator based on magnetic induction for a closed lid thermal cycler (PCR machine). Overall, the experimental yields can be used to build a wireless temperature validator for a sealed PCR machine based on magnetic induction.

Keywords: PCR, magnetic induction, thermal cycler, magnetic hall-effect sensor.

I. INTRODUCTION

Polymerase chain reaction (PCR) is a chemical reaction based on thermal cycling to detect the presence of specific genetic materials (RNA or DNA) from liquid organic material as a sample [1]. The PCR process is divided into 4 phases of reactions based on temperature level. The reactions are denaturation (94°C - 96°C), annealing (45°C - 60°C), extension (76°C), and finishing (0°C - 4°C) [2]. All reactions occur in a PCR test machine known as a thermal cycler. The Thermal cycler works based on the temperature values read by internal temperature sensors inside the machine. This sensor is usually installed inside or on one side of the thermal cycler block [3]. Figure 1 shows the views of the thermal cycler and the composed components inside.

The temperature sensor [4] will degenerate its sensitivity by nature, and this degradation makes the indicator value from the sensor will be drift slowly and less accurate over time. It also means the error value of measured temperature increases due to usage time [5]. For this reason, the thermal cycler needs to be adjusted or fixed based on the measurement using external standard [6] of measurement for certain period. In the case of a thermal cycler, some special measurement techniques needs to be applied to ensure the required heat is well conducted to the sample tube inside PCR machine for each thermal phase of the reactions [3].

In order to reach accuracy and precision, the temperature measurement for thermal cycler cannot be occurr under open-air conditions. A small hole that existed makes the measurement is not accurate anymore. In the case of a thermal cycler, the measurement process needs to close the lid of the thermal cycler and then measures the temperature from the outside of the machines. However, the lid and the case of the thermal cycler retain the heat to the outside of the machine. This condition makes measurement very difficult.

Measuring temperature based on infrared signals [7] might solve the problem, but infrared signals are difficult to penetrate through thicker casings or walls [8]. This makes the heat from the PCR machine not much radiated

* Corresponding Author.
Email: swiv001@brin.go.id
Received: January 18, 2022 ; Revised: June 3, 2022
Accepted: June 6, 2022 ; Published: August 31, 2022

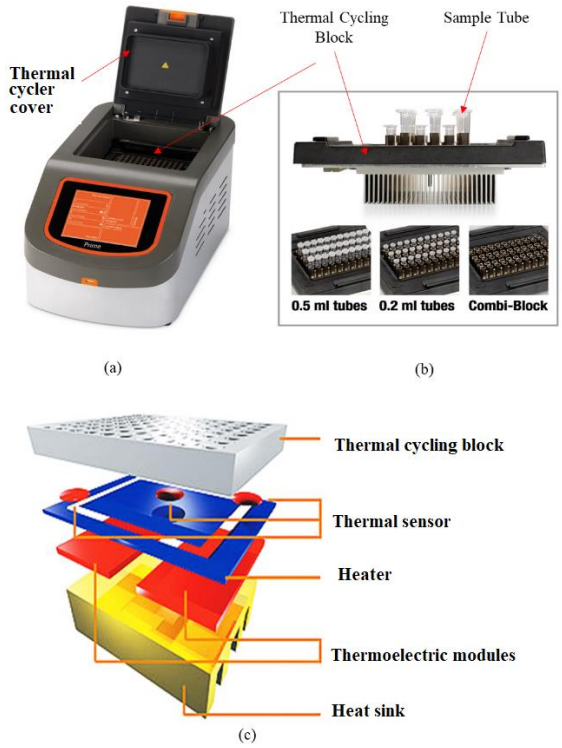

Figure 1. (a) Commercial thermal cycler/ PCR test machine [4]; (b) thermal cycler block with variant of sample tube; (c) inside thermal cycler/PCR test machine

further the infrared signal will be detected at lower levels [9]. Moreover, the infrared sensor signal will be mixed with the infrared signal that radiates from the surface of the hard case of PCR machines [7]. This mixed signal will make ambiguous data during the heating process, and this condition would make the measurement data received from the infrared signal is invalid [8].

Identifying changes in the magnetic flux [9] to the influence of temperature can inspire the discovery of a better method of temperature measurement using an external standard of measurement on the thermal cycler [10]. This study aimed to investigate the relationship between the quantity of the magnetic induction and changes in temperature measurements during the closed lid thermal cycler while running. The results of this study can contribute to the invention of a better thermal cycle validation method for temperature measurement in the closed PCR machine. Moreover, the wireless method can be employed to validate temperature measurement in the closed lid of the PCR machine. Both linearity and measurement uncertainty analysis [11] should be utilized in this work. In addition, the sensitivity of the signal could investigate more dept for this research.

II. METHODOLOGY

A. Temperature Validation Problem on Sealed Thermal Cycler

Generally, the direct method [6] is employed to validate the temperature indicator in the thermal cycler. Some instruments have to be arranged into a system to accommodate this method. This probe is placed and attached to the thermal cycling block. If possible, the probe is not only touched the thermal cycling block but is also immersed in the sample hole. When the heat is generated by the heating systems of the thermal cycler, will distribute to all molecules in the thermal cycling block. At the same time, the sensor probes received the heat transferred and then changed it to the electric signals. This electric signal then propagates to the processing unit of the temperature validatsor through the cables. The signals are filtered from noises in the processing unit and amplified to gain correct temperature values. The results are then displayed to the monitor and recorded manually by the operators in the final steps. Some types of validators automate systems [12] to record the output data in real-time. In this article, the validation system mentioned above is also called a conventional validation system.

The conventional temperature validation system puts the probe inside the thermal cycler.This system connectsthe probe and validator instruments with the cables. The cable propagates the electrical signal from the probe to the processing unit of the temperature validator. The wireless system in the probe might not work correctly inside any heating machine-like thermal cycler, becausethe probe is only effective by using the cables to connect with the validation system. For thermal cycler, using wires on the probe will become a problem. Some thermal cyclers are never working if the PCR cover is not closed tightly. In other words, the conventional validation system is not working correctly for enclosed thermal cyclers.

Only open thermal cycles can use the conventional validation method. Apart from traditional temperature, a validator cable will be pinched when someone tries to validate the enclosed thermal cycler. Theoretically, the cable's resistance value can be considered as the total amount resistances unit value along the cable [5]. Suppose we assume the cable is composed with an amount of a tiny components which the value of resistance (resistant unit) is dR and it bound with geometrical characteristic. In this case, the relation for all resistance unit can be described as (1),

$$R = \sum_{i=0}^{R} R_i = \lim_{l \to 0} \sum_{i=0}^{i=1} \rho \frac{\Delta \vec{l_i}}{\vec{A_i}} = \rho \int_0^l \frac{d\vec{l}}{\vec{A}} \qquad (1)$$

where R means the resistance of cables (Ohm). The resistivity is ρ (Ohm meter), the cross-section surface is A and the length of wires is l, and the unit of measurement is assumed as dl. The sigma notation is described the unit of resistance as serially connected.

Figure 1 gives a simple illustration of this condition. Figure 1 (a) explains how the conventional validation systems potentially damage the temperature validator cables. Figure 1 (b) shows how the pinched wires [8] will change the geometrical characteristics of lines as in (1). There is no choice but to validate the PCR machine test accurately using open-air conditions. A small hole that existed makes the validation not accurate anymore. This means the operator must close the top cover/ PCR plate cover tightly first to turn on the machine. The open-air condition also means when the thermal cycler is not really close. The upper cover or PCR-plate cover still has a gap that makes the leakage of thermal energy. The heat can transfer to the open air like a convection current. The

curl of heating air might be swiveled around the thermal cycler, making the lower temperature in the finishing phase hard to reach. Some thermal cyclers might still work in open-air conditions even if it causes some damage.

Measured temperature determines the next thermal phase of the reaction generated by the program inside the PCR test machine. To gain precise measurement, the sensor has to pass the validation process. For some enclosed PCR types, the validation process needs to be modified. Some operators will open the case to help the validation process. This condition will not become effective because the validation occurs in no real state like PCR machines usually work. This case also does not include the machine's cover and closed environment, which might yield variations of random error. Some PCR machine will not generate heat unless the top surface or particular case is closed, that means the validation process will not be able to modify that the surface is opened.

Indirect measurement will need to accompany the methods of the testing. One of the provided methods is using infrared thermal measurements, which can measure the temperature without physical contact [13], [14]. This method will calculate the temperatures based on the emerging infrared wave [15]. The formula for black body radiation (L) at the wavelength (λ) and temperature (T) is as follows.

$$L = \frac{C_1}{\lambda^5(e^{C_2/\lambda T}-1)} \quad (2)$$

where, first Planck's constant (C_1) is 3,74 * 10 $^{-16}$ Wm^2 and second Planck's constant (C_2) is 1,44 * 10 $^{-2}$ Km.

However, the cover of the PCR machine sometimes insulates the heat inside, because the heat generated by the machines needs to be isolated to make all the electrical systems inside the PCR machine work correctly [7]. This isolation is also created to make zero heat transfer to the environment, making the PCR machine high efficiency. In other words, the heat will be emitted in a small amount from the PCR machine surface to the atmosphere, and the infrared signal will exceed at a lower level as (2). Additionally, the infrared signal on the sensor will be interfered with by the signal emitted from the surface of the PCR machine cover. Therefore, this interference will cause the infrared sensor reading signal inaccurate, making the non-contact temperature measurement method unreliable with an infrared thermometer.

A. Proposed Method

The new method is provided in this attempt which uses Hall-effect as a critical point. The Hall-effect [16] can be used to determine every contactless information using a net of magnetic flux. This method is chosen because anomalous magnetic interaction can interact with or depict the situation inside the hard case of the non-magnetic absorption material, which is usually used in PCR test machines. The magnetic flux is related to the magnetization of material [17]. As a magnetic material's applied temperature elevates, the magnetization will decline [9], because the heat will make the polarization in every particle from the material interfere, and finally, the polarization will be shifted in a random direction [18]. Based on this situation, we can get benefit from magnetization to determine the temperature of the material. Furthermore, the magnetization will lead to a novel method of contactless thermal validation on enclosed PCR test machines.

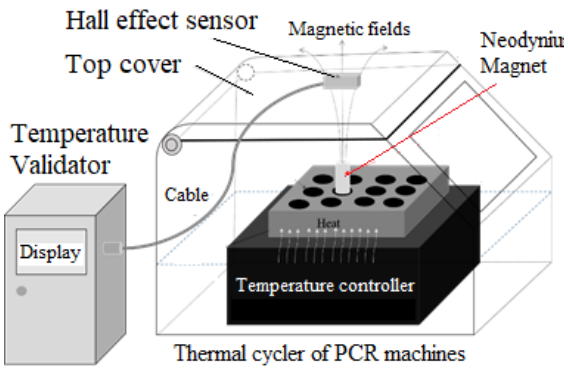

Figure 2. Thermal validation process based on magnetic field detection

Before the complete system for the thermal validation process based on the magnetic field is created, a lab-scale experiment needs to be conducted to verify the method. A small experiment is built to demonstrate this new method of the validation system. In the first step, the investigation is purposed to ensure that the magnetic induction reacts to the temperature changes in a specific environment. The environment is made as close as possible to the conditions when calibrating the enclosed thermal cycler. This experiment needs to provide some KY-024 Linear Magnetic sensor equipment, Max 6675 as thermocouple, Arduino Uno as a microcontroller, neodymium as magnet medium, heating element as heat generator on PCR Well and hard case cover as a wall or casing of PCR machine. The set-up of the experiment is shown in Figure 3.

Linear Hall-effect sensor KY-024 has initial flux magnetic. This flux will interact with another magnetic flux emitted from a neodymium magnet. Furthermore, the Neodymium magnet is utilized as a vector that sends the fluctuated signal for KY-024 based on temperature changes. This fluctuation occurred due to the heat absorbed from the heating element as a heat generator in the PCR machine. The electric current will induce the change of flux magnet, which will read as analog signals in the microcontroller. Then, it will convert the temperature change into electrical potential different in MAX6675 [19]. The electric current will create this potential difference which will transport to the ATmega328P microcontroller of the Arduino Uno board. Both signals are then displayed as a numerical value in PC that will be data of the experiment.

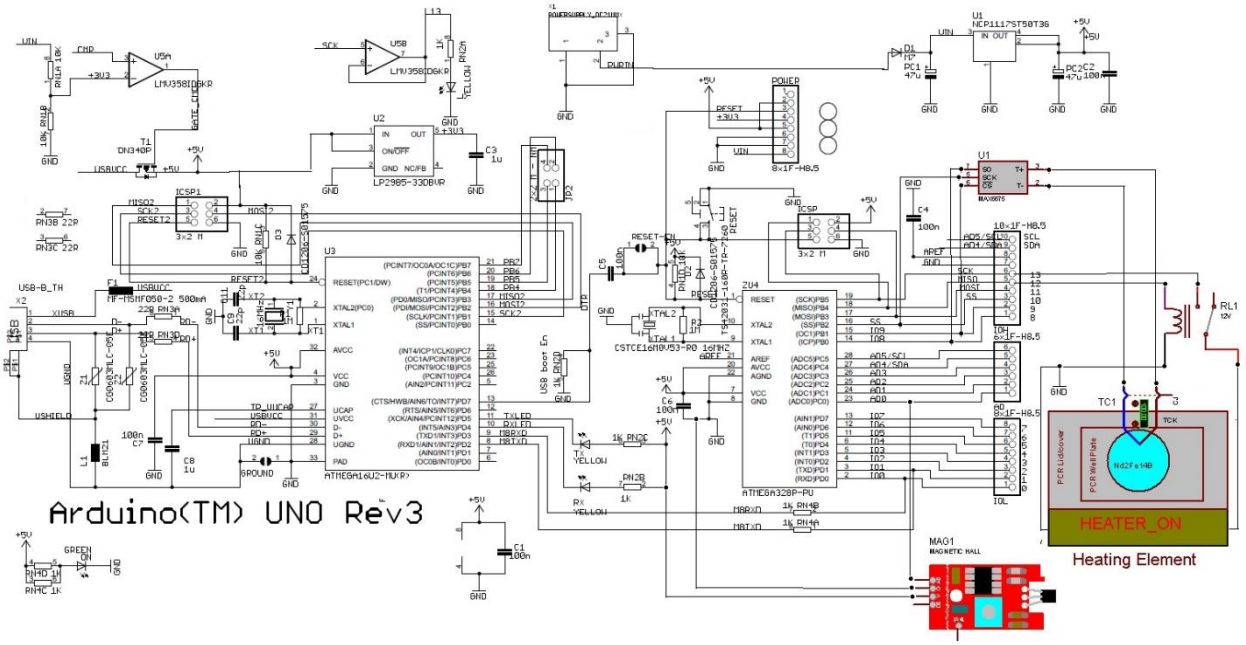

Figure 3. Electronics schematic experiment of temperature validation for enclosed PCR machine using linear Hall-effect sensor

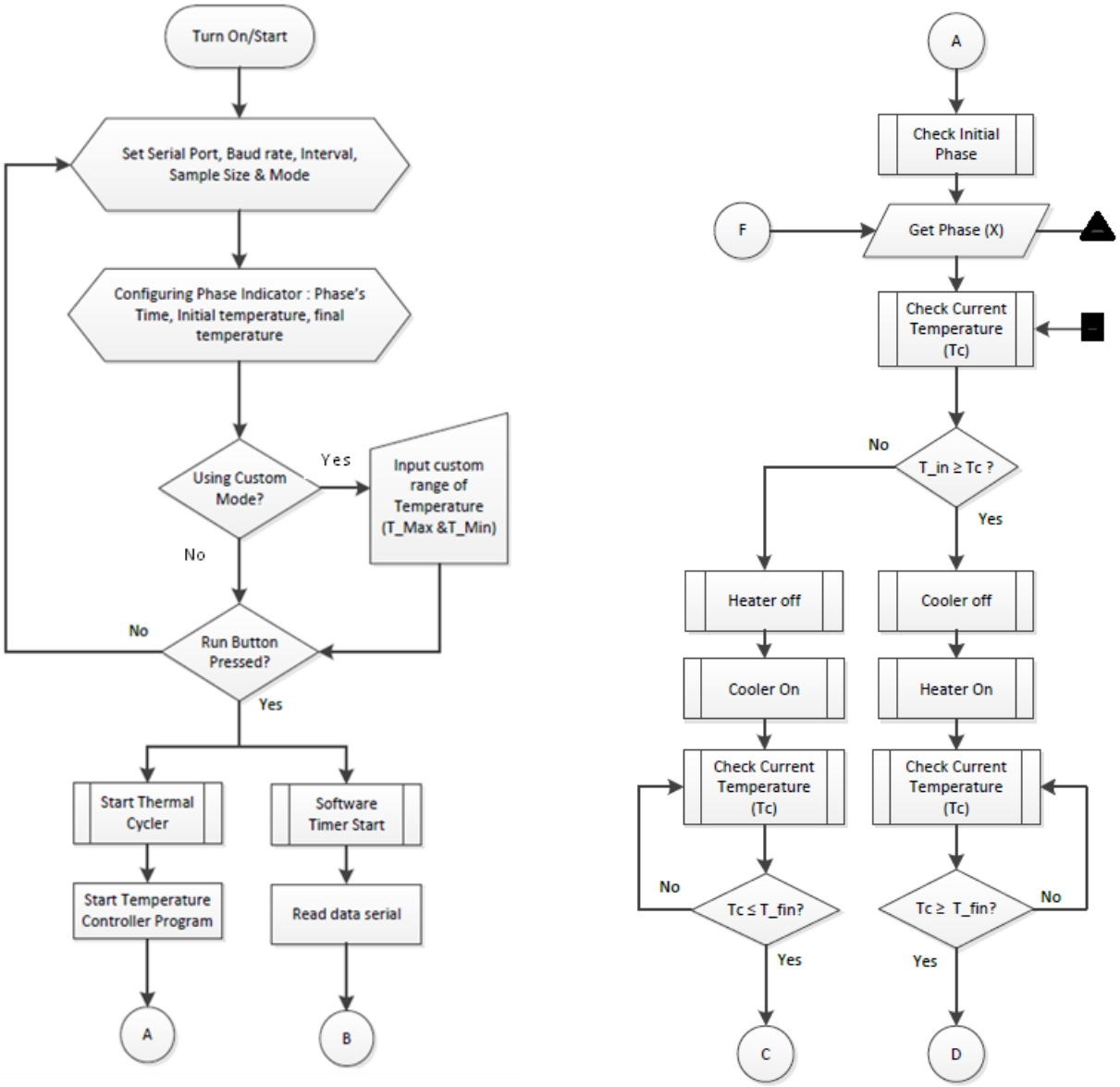

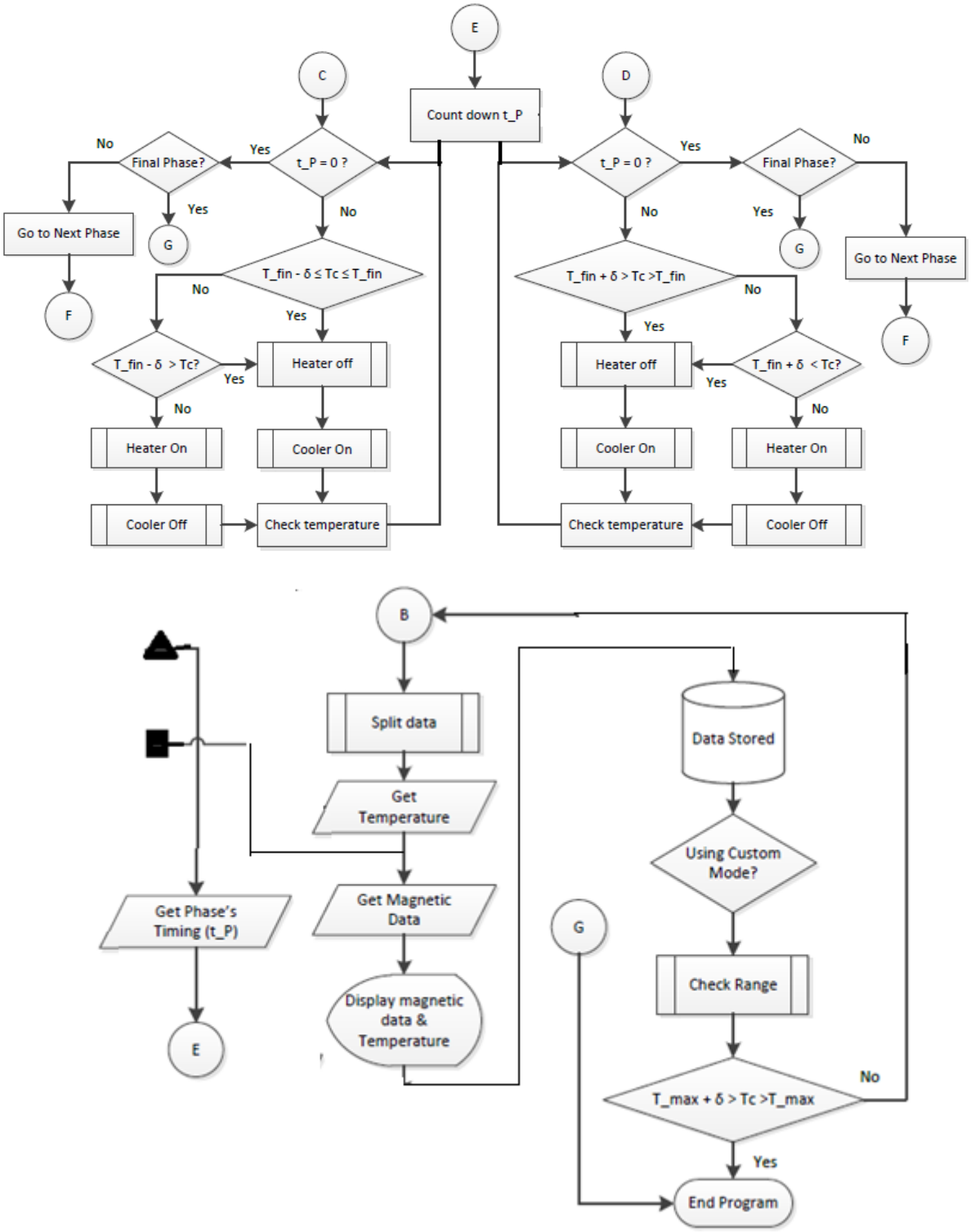

Figure 4. Flow chart of algorithm

The PCR test machine has a graphical user interface (GUI) program. The program is customized and created using the basic visual program to control the simulation and analysis of enclosed-PCR Machine and Thermal Phase Validator Machine or temperature validator. The process begins with turning on the validator machine, and then the GUI program is displayed. The Program will display several forms. For the first step, the users have to set configuration forms. The users must set serial port, baud rate, interval, Sample size, and Mode. In the experiments, the baud rate is set to 9600, the interval is set to 10 seconds, the sample size is set to 10 data, and the mode is average. This machine provides several modes to retrieve the data. But the most recommended is using the intermediate mode, so the mean value of several data will be calculated and displayed on the screen as a single piece of information. The next step is configuring the phase indicator. In this step, the users must determine what PCR Phase they want to validate further for analysis. The denaturation phase is the first phase in the thermal cycler process which is the default

configuration in the phase indicators form. In phase indicators configuration form, the users must also configure the time span for a specific phase in the PCR process, the initial temperature, and the final temperature for each phase. The program also provided a custom mode that uses custom temperature ranges. If the users use custom modes, so the users have to arrange maximum temperature (T_{Max}) and minimum temperature (T_{Min}) in the configuration form. The next step after the configuration is finished is to run the program by pushing the run button. If there is any mistake in configuration, the program will not run, and the user is directed back to the configuration menu. If there is no problem in configuration, the program will start the thermal cycler and start the temperature controller program. At the same time, the program will start the timer and read data by using a serial connection.

The thermal cycler will check the initial phase when the validator program starts to monitor the thermal cycler and get the phase of the thermal cycler at nearly the same time. The program will check the current temperature (T_c) every second. In the denaturation and extension phase, if the temperature is less than or equal to the initial temperature, the cooler will be off, and the heater will be on, so the heating process starts. In the annealing phase and final phase, the heater will be off and the cooler on, so the cooling system starts. The program always checks the current temperature during the heating and heating process, and this process will run until the configured final temperature (T_{fin}) on the current phase has been reached.

In a thermal cycler, there is a steady state in every phase when the temperature reaches the configured final temperature. This condition will hold for a specific time depending on the time configuration of the phase that the user has set. The steady-state maintains the current temperature at a nearly constant value by checking the temperature and controlling the heater and cooler consecutively every second. The current temperature (T_c) must be equal to the Final temperature (T_{Fin}) or has a very small difference (δ) which so-called as the tolerance value. The tolerance must be set on the configuration form before running the thermal cycler.

The maintenance process starts by checking the time phase time (t_P). When the steady-state starts, the program will begin counting the time until zero seconds are left. After the times up, the program will check whether the current phase in the thermal cycler is the final phase or not. If the phase is the final phase, the Program will end the running process of the thermal cycler and the serial monitoring process. If the thermal cycler has yet reached the final phase, the thermal cycler is set to the next phase.

In the validator machine, after the raw data is retrieved, the raw data will split until the temperature value is obtained. The remains will indicate the magnetic data. Both of these values determine the current phase is running, and the machine will get the timing phase information. The data will display on the user interface screen and stored on the device. The program must check the range if stored data is received using the custom mode. If the current temperature data just had a slight difference value (δ) from the maximum temperature, the program will end the data acquisition process. If not, so the program will continue to retrieve the data.

Sensors and measuring instruments must be validated to a precise measurement standard to determine their initial values. Furthermore, the program algorithm for measuring temperature and magnetic induction on the PCR machine's thermal cycler can first be made a flow chart in Figure 4.

The code from the flow chart program will be uploaded in Arduino Uno during the experiment process as a data acquisition controller. Analog signal from magnet sensor is acquired to the internal microcontroller Analog to Digital Conversion (ADC). In addition, the temperature sensor employs Serial Peripheral Interface (SPI) communication. The temperature control is applied by an electronic relay through a digital pin of a microcontroller. The code is arranged for the system to take the data and display it on a PC (Personal Computer) every second. The time indication, temperature value, and magnetic flux data are recorded simultaneously. The temperature will hold this process until the temperature reaches the maximum value required for the denaturation process (94°C - 96°C).

B. Calculation Analysis

The measured magnetic induction, *B*, relates to the temperature measurement, *T*, as (3).

$$B \propto T \tag{3}$$

International standard usually applies measurement uncertainty [20], [21] calculation on calibration [22], [23] and testing report to evaluate stability and repeatability from experimental data. The measured magnetic induction and temperature between probe sensors data as (3) would be assessed its measurement uncertainty to investigate the quality of sensor accuracy following these equations below:

$$\bar{x} = \frac{\sum x_i}{n} \tag{4}$$

$$s = \sqrt{\frac{\sum (x_i - \bar{x})^2}{n-1}} \tag{5}$$

$$u_{i-n} = \frac{s}{\sqrt{n}} = \frac{\sqrt{\frac{\sum (x_i - \bar{x})^2}{n-1}}}{\sqrt{n}} \tag{6}$$

$$c_i = \frac{\delta B}{\delta \bar{x}} \tag{7}$$

$$u_c = \sqrt{\sum c_i^2 . u_i^2} \tag{8}$$

$$U_{ex} = k . u_c \tag{9}$$

where $\bar{x}$ being measurement uncertainty data-i from repeatability; u_{i-n} being measurement uncertainty

data-i from repeatability; *s* being standard deviation; x_i being data of *i*-th value; *n* being number of data; u_i being standard measurement uncertainty; u_c being combined uncertainty; c_i being sensitivity coefficient; *s* being standard deviation; x_i being data of *i*-th value; *n* being number of data; *k* being coverage factor; U_{ex} being expanded uncertainty.

Linearity of digital signal due to (3) can be modeled as (10) below. The output (*y*) signal of the measured voltage is caused by the temperature as input (*x*), in which a and b are constant.

$$y = a + b \times x \Rightarrow T = a + b \times B \quad (10)$$

The coefficient of determination (R^2) is implemented to assess the quality of signal linearity. R^2 represents the fit a linear function model (f_i) on (11) to the experimental data. The value by 1 stated that the signal has perfect linearity. On the other hand, the R-squared value has the worse linearity at 0.

$$R^2 = 1 - \frac{\sum_i (y_i - \bar{y})^2}{\sum_i (y_i - f_i)^2} \quad (11)$$

The excellent linearity tends to have uniform sensitivity (ς) for every measuring point. The ratio between output and input ($\Delta y/\Delta x$) indicates its sensor sensitivity.

$$\varsigma = \frac{\Delta T}{\Delta B} \quad (12)$$

III. Results and Discussion

The gauss meter was used to validate the voltage input from the ADC of a microcontroller. The distance variation between the Neodymium magnet and the sensor is applied to produce different magnetic induction measuring points. Furthermore, the gauss meter is utilized to ensure the actual value of magnetic induction, which is read by a microcontroller.

Interestingly, the voltage input of microcontroller achieved excellent linearity (R^2=0.9779) with the magnetic flux so it can support our experiment.

The validation experiment used two pieces of neodymium magnets (20 x 5 x 1.5 mm) which were similar to each other. The distance is set around 0.5 cm. The experiment yielded the data depicted as graphics in Figure 7.

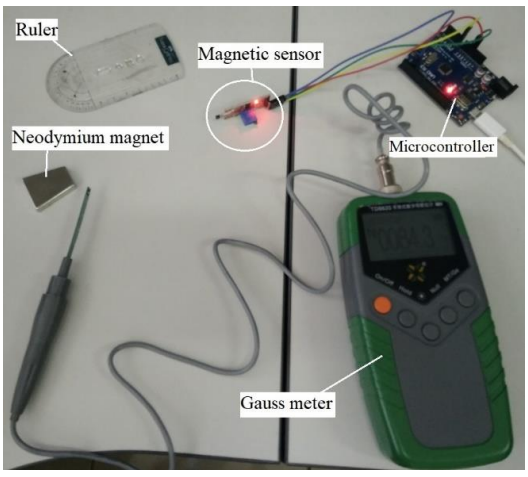

Figure 5. Magnetic sensor measurement validation by gauss meter

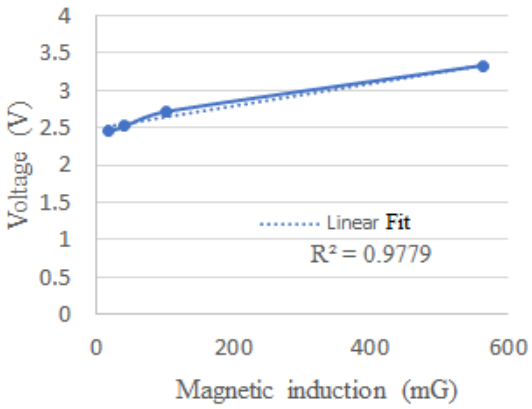

Figure 6. Temperature value vs magnetic flux

The experimental results in the graph in Figure 7 prove that temperature changes affect the quantity of the magnetic induction accordingly. The greater the increase in temperature in the PCR machine, the greater the magnetic flux value, which shows a proportional relationship in (3). The coefficient of determination (*R*) on (11) is 0.7794 from the result of the linear function modelled accordingly (10). The mean values in (4) and the expanded uncertainty in (9) were estimated to investigate the measurement results in depth in Table 1. In addition, sensitivity analyzes were calculated accordingly (12) to observe the linearity.

Table 1 showed the mean value of magnetic flux increases with rising temperature. The smallest

Table 1
Magnetic flux Results of normal pole

Thermal Phase	Normal Pole (repelled each other)		
	B (mG)	Uex (mG)	ς (°C /mG)
Annealing (45°C - 60°C)	524.5	0.1	0.0649
Extension 76°C	526	0	0.0255
Denaturation (94°C - 96°C)	526.5	0.7	-

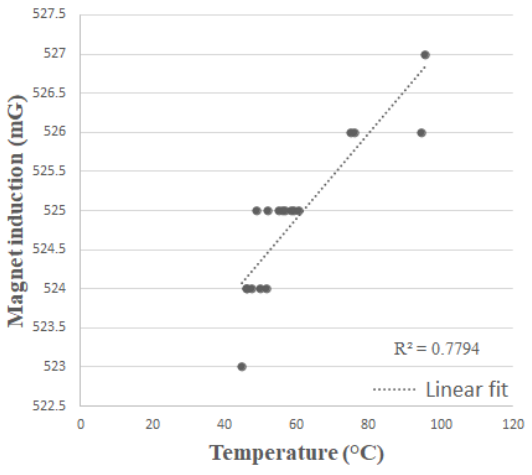

Figure 7. Temperature value vs magnetic flux

measurement uncertainty value by 0 mG occurred at a temperature of 76°C. However, the denaturation thermal phase had the largest expanded uncertainty of 0.7 mG. Furthermore, the measurement uncertainty at a temperature from 45°C to 60°C happened at 0.1 mG. The difference in sensitivity also illustrated that the relationship between magnetic induction and temperature was not precisely linear by 0.0649 and 0.0255 °C /mG, respectively.

Table 1 showed the mean value of magnetic flux increases with rising temperature. The smallest measurement uncertainty value by 0 mG occurred at a temperature of 76°C. However, the denaturation thermal phase had the largest expanded uncertainty of 0.7 mG. Furthermore, the measurement uncertainty at a temperature from 45°C to 60°C happened at 0.1 mG. The difference in sensitivity also illustrated that the relationship between magnetic induction and temperature was not precisely linear by 0.0649 and 0.0255 °C /mG, respectively.

At the initial, flux magnetic emitted from two objects, KY-024 and neodymium magnets, repelling each other. When the temperature applied in the heating element is increased, the flux of the neodymium magnet attached above the heating element decreases. This also means the neodymium magnet vanished its magnetization slowly. In the 65°C - 94 °C, the sensor displayed the value of flux magnetic around 527-528 mG. This wide range will make it challenging to determine representative magnetic flux value as a standard validation value on a certain phase of PCR.

When the pole of the magnet is reversed (Initial magnetic flux in the same direction with KY-024 initial magnetic flux), the data experiment shown that the increase of temperature decreases the magnetic induction. On the other hand, this result is inversely symmetrical to the previous magnetic pole pattern results. This data is represented in the graphic Figure 8.

Fascinatingly in Figure 8, the results of magnetic flux measurements at the reversed pole position had a decreasing trend with growing temperatures, diverse from the previous magnetic pole pattern in Figure 8.

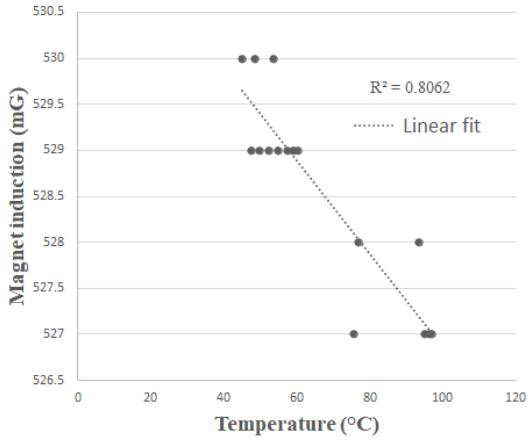

Figure 8. Temperature value vs magnetic flux in reversed magnetic pole

TABLE 2
MAGNETIC FLUX RESULTS OF REVERSED POLE

Thermal Phase	Normal Pole (repelled each other)		
	B (mG)	Uex (mG)	ς (°C /mG)
Annealing (45°C - 60°C)	529.3	0.1	-0.0769
Extension 76°C	527.5	0.7	-0.0130
Denaturation (94°C - 96°C)	527.3	0.3	-

The R^2 value was better than the last position by 0.8062. The coefficient of determination indicated the linearity of the relationship between magnetic induction and temperature was more suitable at the reserved pole position. Figure 8 verified previous research on Neodymium magnets in [9].

The reversed magnetic pole experiment demonstrated more uncertainty in the extension of the thermal phase by 0.7 mG. However, denaturation had better measurement uncertainty. Furthermore, the sensitivity and gradient of the curve had negative values. Nevertheless, this position has slightly more linearity according to the coefficient of determination.

Each magnetic pole position had its advantages according to the thermal phase. Table 3 described the proposed magnetic pole position for validating temperature measurements on a closed thermal cycler of the PCR machine.

The experimental data in Figure 7 and Figure 8 can be manipulated to develop a prototype temperature

TABLE 3
PROPOSED MAGNETIC POLE POSITION

Thermal Phase	The best magnetic pole position
Annealing (45°C - 60°C)	Reserved pole
Extension 76°C	Normal pole
Denaturation (94°C - 96°C)	Reserved pole

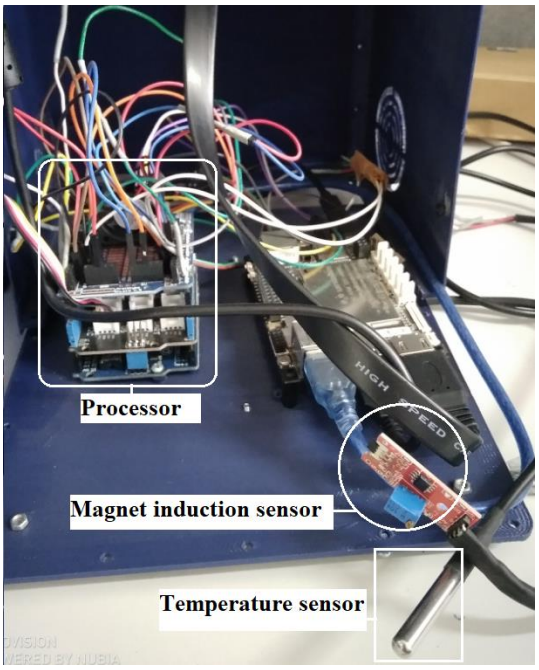

Figure 9. prototype of temperature validator for closed PCR machine based on magnetic induction

validator [24] on a sealed thermal cycler of PCR machine according to the influence of the magnetic induction relationship in Figure 9. Furthermore, the electronic circuit in Figure 3 was realized on the temperature validator in retrieving experimental data.

Hence, the proposed non-contact validator for temperature measurement in a sealed PCR machine by magnetic flux technique could be a solution for problems in (1) and (2) before through wireless technique. The relationship between temperature [25] and magnetic induction can inspire application in other research fields.

IV. CONCLUSION

The results of the investigation of magnetic induction measurements on temperature, which was successfully verified by gauss meter, on a closed thermal cycler of PCR machine showed a relationship between the two which depends on the position of the magnetic poles. For the normal pole or magnetic conditions repelled each other, the greater the temperature, the larger the magnetic flux measured. On the other hand, the inverse relationship between magnetic induction and temperature occurred at the reversed pole position, which is in the same direction. The best measurement uncertainty generally occurred in the annealing process by 0.1 mG.

Therefore, the experimental results can develop a wireless temperature validator for a closed PCR machine based on magnetic flux. From the measurement uncertainty analysis and signal sensitivity results, the position of the reversed pole magnet is recommended at the annealing stage. In comparison, the thermal phase extension can use the normal pole position. Furthermore, the denaturation stage should take advantage of the reversed pole position.

DECLARATIONS

Conflict of Interest

The authors have declared that no competing interests exist.

CRediT Authorship Contribution

Swivano Agmal: Software, Data curation, Writing-Original draft preparation, Jalu Ahmad Prakosa: Methodology, Writing-Reviewing Editing, Agus Sukarto Wismogroho: Conceptualization, Supervision, Funding Acquisition.

Funding

Research reported in this publication was supported by IPT-LIPI project and Ministry of Finance through Rispro-LPDP Konsorsium 2021.

Acknowledgment

The team of authors is grateful to management of National Research and Innovation Agency of Republic Indonesia BRIN) in the framework IPT-LIPI project and Ministry of Finance through Rispro-LPDP Konsorsium for supporting this research.

REFERENCES

[1] Y. M. D. Lo and K. C. A. Chan, "Introduction to the polymerase chain reaction," *Clin. Appl. PCR*, pp. 1–10, 2006, doi: 10.1385/1-59745-074-X:1.

[2] M. Joshi and J. D. Deshpande, "Polymerase chain reaction: methods, principles and application," *Int. J. Biomed. Res.*, vol. 2, no. 1, pp. 81–97, 2011. [Online]. Available: http://www.ssjournals.com/index.php/ijbr/article/view/640

[3] D.-S. Lee, "Real-time pcr machine system modeling and a systematic approach for the robust design of a real-time pcr-on-a-chip system," *Sensors*, vol. 10, no. 1, pp. 697–718, 2010. doi: 10.3390/s100100697.

[4] A. A. Abouellail, I. I. Obach, A. A. Soldatov, P. V Sorokin, and A. I. Soldatov, "Research of thermocouple electrical characteristics," in *Mater. Sci. Forum*, 2018, vol. 938, pp. 104–111. doi: 10.4028/www.scientific.net/msf.938.104.

[5] J. A. Prakosa, D. Larassati, and others, "Development of simple method for quality testing of pt100 sensors due to temperature coefficient of resistance measurement," in *2021 Int. Symp. Electron. Smart Devices*, Bandung, 2021, pp. 1–5. doi: 10.1109/ISESD53023.2021.9501552.

[6] J. A. Prakosa, C. M. Su, W. B. Wang, B. H. Sirenden, G. Zaid, and N. C. E. Darmayanti, "The traceability improvement and comparison of bell prover as the indonesian national standard of gas volume flow rate," *Mapan - J. Metrol. Soc. India*, vol. 36, pp. 81-87, 2020, doi: 10.1007/s12647-020-00402-4.

[7] P. Wegierek and M. Konarski, "The temperature effect on measurement accuracy of the smart electricity meter," *Prz. Elektrotechniczny*, vol. 92, no. 8, pp. 148–150, 2016. doi: 10.15199/48.2016.08.40.

[8] B. R. Lyon Jr, G. L. Orlove, and D. L. Peters, "Relationship between current load and temperature for quasi-steady state and transient conditions," in *Thermosense XXII*, 2000, vol. 4020, pp. 62–70. doi: 10.1117/12.381580.

[9] M.-D. Calin and E. Helerea, "Temperature influence on magnetic characteristics of ndfeb permanent magnets," in *2011 7th Int. Symp. Adv. Top. Electr. Eng.*, Bucharest, 2011, pp. 1–6. [Online]. Available: https://ieeexplore.ieee.org/abstract/document/5952212.

[10] C. Anwar, E. S. Rosa, S. Shobih, J. Hidayat, and D. Tahir, "Analysis of thermal treatment zirconia as spacer layer on dye-sensitized solar cell (dssc) performance with monolithic structure," *Jurnal Elektronika dan Telekomunikasi*, vol. 18, no. 1, pp. 21–26, 2018. doi: 10.14203/jet.v18.21-26.

[11] S. Agmal, J. A. Prakosa, and C. Astuti, "Measurement uncertainty analysis of the embedded system of microcontroler for an accurate timer/stopwatch," in *2021 7th Int. Conf. Electr. Electron. Inf. Eng.*, 2021, pp. 290–294. doi: 10.1109/ICEEIE52663.2021.9616813.

[12] K. S. Chong, N. A. Devi, K. B. Gan, and S.-M. Then, "Design and development of polymerase chain reaction thermal cycler using proportional-integral temperature controller," *Malaysian J. Fundam. Appl. Sci.*, vol. 14, no. 2, pp. 213–218, 2018. doi: doi.org/10.11113/mjfas.v14n2.765.

[13] G. S. Marchini *et al*., "Infrared thermometer: an accurate tool for temperature measurement during renal surgery," *Int. braz j urol*, vol. 39, pp. 572–578, 2013. doi: 10.1590/S1677-5538.IBJU.2013.04.16.

[14] S. Masoudi, M. A. Gholami, J. M. Iariche, and A. Vafadar, "Infrared temperature measurement and increasing infrared measurement accuracy in the context of machining process," *Adv. Prod. Eng. \& Manag.*, vol. 12, no. 4, pp. 353–362, 2017. doi: 10.14743/apem2017.4.263.

[15] H. Wiriadinata, "Termometer inframerah: teori dan kalibrasi,", Indonesia: LIPI Press, 2015.

[16] A. A. Ali, G. Yanling, and C. Zifan, "Study of hall effect sensor and variety of temperature related sensitivity," *J. Eng. Technol. Sci*, vol. 49, no. 3, pp. 308–321, 2017. doi: 10.5614/j.eng.technol.sci.2017.49.3.2.

[17] P. Zhou, D. Lin, Y. Xiao, N. Lambert, and M. A. Rahman, "Temperature-dependent demagnetization model of permanent magnets for finite element analysis," *IEEE Trans. Magn.*, vol. 48, no. 2, pp. 1031–1034, 2012. doi: 10.1109/TMAG.2011.2172395.

[18] F. Shir, E. Della Torre, L. H. Bennett, C. Mavriplis, and R. D. Shull, "Modeling of magnetization and demagnetization

in magnetic regenerative refrigeration," *IEEE Trans. Magn.*, vol. 40, no. 4, pp. 2098–2100, 2004. doi: 10.1109/TMAG.2004.832475.

[19] S. P. Nalavade, A. D. Patange, C. L. Prabhune, S. S. Mulik, and M. S. Shewale, "Development of 12 channel temperature acquisition system for heat exchanger using max6675 and arduino interface," in *Innov. Des. Anal. Dev. Pract. Aerosp. Automot. Eng. (I-DAD 2018)*, Springer, 2019, pp. 119–125. doi: 10.1007/978-981-13-2697-4_13.

[20] J. A. Prakosa, A. V. Putov, and A. D. Stotckaia, "Measurement uncertainty of closed loop control system for water flow rate," 2019, pp. 60-63. doi: 10.1109/SCM.2019.8903681.

[21] T. Kristiantoro, N. Idayanti, N. Sudrajat, A. Septiani, D. Mulyadi, and others, "Uncertainty measurement on the characteristics of permanent magnet materials using permagraph measuring instruments," (in Indonesia), *Jurnal Elektronika dan Telekomunikasi*, vol. 16, no. 1, pp. 1–6, 2016. doi: 10.14203/jet.v16.1-6.

[22] M. Kok, J. D. Hol, T. B. Schön, F. Gustafsson, and H. Luinge, "Calibration of a magnetometer in combination with inertial sensors," in *2012 15th Int. Conf. Inf. Fusion*, 2012, pp. 787–793. [Online]. Available: https://ieeexplore.ieee.org/document/6289882.

[23] E. Dorveaux, D. Vissière, A.-P. Martin, and N. Petit, "Iterative calibration method for inertial and magnetic sensors," in *Proc. 48h IEEE Conf. Decis. Control held jointly with 2009 28th Chinese Control Conf.*, 2009, pp. 8296–8303. doi: 10.1109/CDC.2009.5399503.

[24] K. H. Sanjaya *et al.*, "Low-cost multimodal physiological telemonitoring system through internet of things," *Jurnal Elektronika dan Telekomunikasi*, vol. 21, no. 1, pp. 55–63, 2021. doi: 10.14203/jet.v21.55-63.

[25] S. Wijonarko *et al.*, "Empirical formulas between outdoor temperature and humidity," in *2021 7th Int. Conf. Electr. Electron. Inf. Eng.*, 2021, pp. 1–6. doi: 10.1109/ICEEIE52663.2021.9616692.